Clinic Rev Bone Miner Metab (2014) 12:66–76
DOI 10.1007/s12018-014-9166-5

ORIGINAL PAPER

Imaging Mechanical Muscle–Bone Relationships: How to See the Invisible

Jörn Rittweger · José-Luis Ferretti

Published online: 4 April 2014

Abstract The ontogenetic adaptation of bones to their habitual loads offers a rationale for imaging muscle–bone relationships. Provided that bones adapt to strains that are chiefly determined by muscle contractions, information from muscle and bone scans allows comparing measures of bone stiffness and strength with surrogate measures for muscular force generation. Prediction of the mechanical behavior of bone is nowadays well possible by peripheral quantitative computed tomography (pQCT). However, prediction of muscle forces is not currently feasible. pQCT offers the opportunity to outline gross muscle cross-sectional area (CSA) as a surrogate measure of the force-generating capacity of muscle groups. Ultrasound and magnetic resonance (MR) imaging allow identification of single muscles. In addition, ultrasound also offers the possibility to assess muscle architecture and thus to assess physiological CSA as a more likely predictor of muscle forces than anatomical CSA. Although there is currently no single technique in use to simultaneously assess muscle volume, CSA, and architecture at the level of single muscles, this could in future be possible by MR diffusion imaging. Current attempts to quantify muscle "quality" are not directly related to the force-generating capacity and thus only of indirect help. Hence, one should hope that better imaging assessments of muscle will be possible in future. However, despite these current limitations, muscle–bone strength indicators have been defined that can already be used today in order to differentiate primary and secondary bone disorders thus underlining the validity of the "muscle–bone" approach.

Keywords Mechano-adaptation · Mechanostat · Bone disorders · Muscle disorders

Abbreviations

BMC	Bone mineral content
CSA	Cross-sectional area
CT	Computed tomography
DXA	Dual energy X-ray absorptiometry
MBSI	Muscle–bone strength index
MM	Muscle mass
MRI	Magnetic resonance imaging
pQCT	Peripheral quantitative computed tomography
QCT	Quantitative computed tomography

Presentation of the Problem(s)

To image muscle–bone relationships makes use of the "form follows function" principle [1]. It assesses the natural process of bone's mechano-adaptation, which is a curious circle of information transductions. Muscles exert forces on bones as *physical* stimuli, which are transduced into *chemical* signals within the bone tissue and then transformed to *geometrical* changes in bone structure which modify its *physical* properties. As with all physiology, understanding is expedited by quantitative analysis.

Naturally, we cannot directly see these forces, or torques, but we can observe their effects and thus reason about their origin. This is best done within the framework of the

J. Rittweger (✉)
Institute of Aerospace Medicine, German Aerospace Center (DLR), Linder Höhe 1, 51147 Cologne, Germany
e-mail: joern.rittweger@dlr.de

J.-L. Ferretti
Center of P-Ca Metabolism Studies (CEMFoC), Faculty of Medicine, National University of Rosario, Rosario, Argentina

physical discipline of mechanics. We are likewise "blind" to the logic behind feedback control systems. Here, the framework is provided by the engineering discipline of cybernetics. Frost's *mechanostat* theory [2] is departing from this framework to explain bone's mechano-adaptation as a homeostatic feedback mechanism. The proposition is that the *mechanostat* aims at keeping bone strains invariant under variant forces by adapting the bone's structure. The often used analogy is a thermostat that controls room temperature by adjusting the radiator power to match variable heat drains.

Thus, imaging muscle and bone relationships can be broken down into four steps.

1. *Assessment of bone properties*: It is important here to consider the mechanically passive nature of bone. Through the technological advancement of the past decades, it is nowadays very well possible to predict the passive mechanical behavior of bones [3, 4].
2. *Assessment of muscle forces*: Within the muscle–bone unit, muscles are the active elements that generate forces. Unfortunately, the muscle forces are not currently measureable by imaging techniques and one therefore has to measure them in an alternative way, or to rely upon surrogate measures of "muscle strength," e.g., the cross-sectional area (CSA).
3. *Identification of muscle–bone strength relationships*: Muscles can impose different kinds of loads upon bones, such as compression, torsion and bending loads. To describe the bone's resistance against these loads, one can assess different structural measures, such as cross-sectional area, or the polar and axial cross-sectional moments of inertia (pCSMI and aCSMI, respectively). Plotting appropriate measures of bone resistance against appropriate measures of muscle strength can then yield certain relationships. Provided they are well interpretable, one can then derive muscle–bone strength indices from these relationships.
4. *Interpretation of muscle–bone strength indices (MBSI)*: Once an MBSI has been established, cutoff values can be defined. This can help to identify cases in which the bones are too feeble for the existing musculature (reduced bone:muscle:bone), which indicates a disorder of bone adaptation. In other cases, feeble bones might be well adapted, as indicated by a "normal" MBSI. Here, one should think of a primary muscle disorder.

Please note that the first 3 steps are normative, i.e., based on technical–mathematical principles, while the fourth step of descriptive nature. Seeing the "invisible" muscle–bone relationships thus largely depends on how well the transition between normative and descriptive levels is achieved.

Figure 1 gives an illustration of the general rationale behind muscle–bone imaging, and the following text will provide an overview of its current status. It can serve to apply the principles in nowadays clinical practice, but also to perceive the areas where improvements might still be needed.

Assessment of Bone Properties from Image Analyses

"Bone mineral density" (BMD) is, physically speaking, an often misleading term. This is because BMD is neither a direct measure for either bone "mass," nor for "quality" or for "strength." Moreover, one has to consider whether it refers to the bone mineral content (BMC) determined in cortical, trabecular or total mineralized tissue in true bone cross-sections ("volumetric" determinations) or whether one is to deal with areal projects, as in dual energy X-ray absorptiometry (DXA). Properly speaking, (1) The DXA-assessed, "areal" BMD (the classical "BMD," in mass/area units) is just the amount ("mass") of mineral contained per unit of projected bone area; (2) The "volumetric" BMD (vBMD, in mass/volume units) of total or trabecular bone determined by quantitative computed tomography (QCT), peripheral QCT (pQCT), high-resolution pQCT (HR-pQCT) or similar techniques in cross-

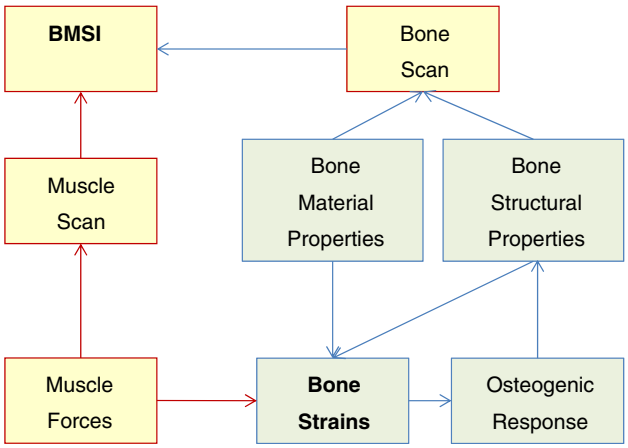

Fig. 1 Rationale for muscle–bone imaging: *arrow* directions indicate the flow of information. *Blue boxes* indicate the bone part. Bone strains play a central role. As predicted by the *mechanostat* theory (and other homeostatic theories of bone adaptation), they define osteogenic responses that lead to structural adaptations. Bone material properties are likely not changed by such osteogenic responses in a homeostatic way. Bone material and structural properties, and acting forces define the bone strain history. For the sake of the current article, the focus is here on muscle forces acting on the bone. Provided that scanning techniques allow identification of muscle force surrogates and bone properties, one can arrive at the assessment of so-called muscle–bone strength indices (MBSI). Please note that this rationale is mainly of normative nature and that only the evaluation of MBSI is a descriptive and empirical exercise (Color figure online)

sectional bone slices are estimates of the mineral "mass" per volume unit of the studied trabecular or total bone; and (3) Particularly, the vBMD of cortical bone (vBMD.Ct) is not actually an estimate of the mineral "mass," but of the mineral *concentration* within the cortical (i.e., "solid") bone tissue. Thus, DXA-BMD and cross-sectional *total* and *trabecular* vBMD's are "extensive variables," surrogates of bone tissue "mass," while the vBMD.Ct is an "intensive variable," surrogate of bone tissue "quality." In fact, the calcium content of the "solid" bone tissue (which is an analogous of the vBMD.Ct) is a well known correlate of the *intrinsic stiffness* ("elastic modulus") of the "solid" mineralized tissue [5].

Concerning compression stress analyses, both trabecular and cortical *masses* are relevant to bone strength, yet the connectivity and directionality of the trabecular network's structural properties are also believed to play a significant role. However, when bending or torsion stresses in long bone shafts are concerned, bone strength is rather determined by both the vBMD and the spatial distribution of the cortical tissue, as surrogates of its intrinsic stiffness (elastic modulus) and of the mechanical efficiency of the bones' architectural design, respectively. The mechanical efficiency of the diaphyseal design can be described by the cross-sectional *second moments of inertia* (MI's, Fig. 2) concerning bending or torsion [6]. Accordingly, the structural stiffness of a long bone diaphysis can be approached noninvasively by the computing the product between vBMD.Ct and MI to yield so-called bone strength indices (BSIs [3]) and the "stress–strain index," SSI [7].

Interestingly, bone tissue "distribution" and "quality" are likely interlinked feedback variables. In fact, the former empirically behaves as functionally associated with the latter following negative, hyperbole-like functions (which we named "distribution/quality," or *d/q* relationships [8]) in many bones, with a high bone site specificity. An intuitive analogy to the *d/q* relationships would be the dilemma between affording high quality building materials and contracting a good architect when budgeting for a house construction. Reasonably, the *d/q* relationships could be regarded as describing the reactive, modeling-dependent distribution of the mineralized tissue as a function of its local intrinsic stiffness as a result of the regulatory work of bone *mechanostat,* with the proposed "objective" to control the structural stiffness of every bone. As long as the bone *mechanostat* reacts to the sensing of the usage-derived strains of bone tissue by osteocytes, it follows that the system would control bone structural properties as a function of the habitual usage of the bones in every skeletal site. Hence, the regional muscle contractions, here assumed as the chief determinants of bone strains throughout the skeleton, constitute the main mechanical input to the bone *mechanostat*.

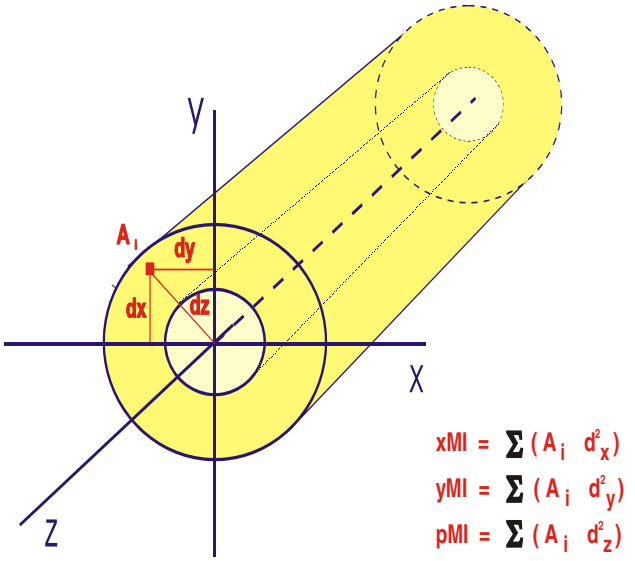

Fig. 2 Conceptualization of the cross-sectional moments of inertia (CSMI, or MI). Each bone cross-section is composed of a number of area elements A_i, and the total CSA is thus the sum of all these elements ($=\Sigma A_i$). For the CSMIs, one has also to consider the distribution, meaning each elements distance from the neutral axis. The neutral axis is defined as the strand that is unstrained during bone loading. In this diagram, it coincides with the *Z*-axis, and it serves as the reference point for coordinates d*x* and d*y*. Three-point bending by forces aligned to the *A*-axis will let the neutral axis curve around the *X*-axis thus leading to shortening along the *Z*-axis on one side of the beam and lengthening on the other. Each area element resists the *Z*-axis shortening in proportion to dy^2. Thus, the CSMI for *y*-bending is given by the sum of products of each elements area and d^2

All the above considerations concern the bones' behavior as *elastic* structures, i.e., under the assumption that all deformation energy is returned and no damage or heat have been dissipated within the bone. Crack production, instead, leads to *plastic* deformation, thus retaining some degree of permanent deformation as a typical pre-fracture behavior. The biological determinants of the elastic behavior of bones are the intrinsic stiffness and the distribution of their mineralized tissue. The plastic behavior of bones depends, in addition, on the bone tissue resistance to the development and progress of cracks within the bone's structure, a property known as bone *toughness*. In this regard, micro-structural "discontinuities" within the cortical "solid" bone tissue such as micropores, lacunae, secondary osteons and *microdamage* can behave as "stress raisers" during the plastic behavior prior to fracture and hence reduce bone toughness. Noteworthy, all these factors are unrelated to bone "mass," mineralization, or distribution, though a high degree of bone tissue mineralization or an altered "crystallinity" can increase bone tissue brittleness. Incidentally, bone tissue's stiffness and toughness seem to have been subjected to some "trade-off" during evolution as an apparent result of a natural "search for the

optimal degree of tissue mineralization" for all vertebrate skeletons, with interesting biomechanical derivations [5].

Surrogate Measures for Muscle Forces from Image Analyses

Bones are loaded by weight, mass-inertial forces and regional muscle forces. Of these, the latter must be expected to generate the by far largest loading contribution [9]. Following the engineering principle that a bridge should be designed for the peak loads, rather than the number of passengers, it seems opportune to identify muscle forces as the chief determinant of bone's mechano-adaptation. Following this simple logic, the main interest will lie in the peak force that muscles can produce. This peak force is often assessed as "muscle strength," usually obtained in maximum voluntary contractions (MVC). One would intuitively think that measuring muscle strength MVC is straightforward, but there are some persistent problems associated with it. Firstly, MVC testing is a functional test that requires volition, and thus an arbitrary element, both from the side of the tester and of the tested. Second, most MVC dynamometers apply forces in unusual places, i.e., in the shin for knee extension testing. The question thus arises how accurate these measurements are, and how we know that all people can tolerate such testing conditions equally well. Thirdly, as explained below (see "co-contractions" in subsection "complexity of the musculature") it is questionable, in practice, whether peak forces are produced during MVC testing, or whether more complex, ballistic movements cause greater muscle forces. This opens the general question of validity: Even if we could perform MVC testing with high precision and accuracy, how convinced are we that MVC testing is representative of those habitual loads that have shaped a particular bone?

Muscle CSA as an Indicator of Force

It is generally held in exercise and muscle physiology that of the different "size" properties of a muscle, it is the CSA that represents its force-generating capacity. This is because force generated by a muscle is the sum of all sarcomeres in parallel, and the CSA is directly related to their total number. There is also a slightly different view angle of this that has to do with the mechano-adaptions of muscles. As illustrated in Fig. 3, one can subdivide the habitual loading history of the muscle–bone unit into such stimuli that affect both muscle and bone (intersection in Fig. 3), and others that either affect bone only or muscle only. The crucial point now is that peak forces clearly are the chief determinant for muscle size [10], and that peak

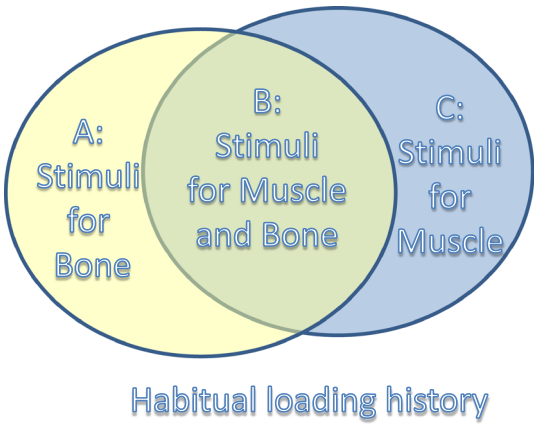

Fig. 3 Rationale for using muscle size as representative surrogate measure: The musculoskeletal system's habitual loading history can theoretically be subdivided into such stimuli that affect both muscle and bone (=intersection *B*), and such stimuli that either affect muscle only (*set A*) or bone only (*set C*) or both. The larger intersection *B*, the more it will be possible the more appropriate it will be to deduce habitual bone loads from muscle size measurements. Of note, peak forces are a major determinant for muscle size and bone size and distribution

strains, which are in obvious relation to these peak forces, are the principle determinant for bone adaptation [11, 12]. Moreover, it is known that force rate and strain rate are in themselves potent stimuli to muscle and bone [10, 13]. In other words, both muscle size and bone mineral content (BMC) and distribution are largely determined by one factor, namely peak force. In this sense, muscle CSA not only is indicating a muscle's capacity to generate force, it probably is also a reflection of that part of the musculoskeletal loading history that is most relevant to bone. Of course, we know that some stimuli are meaningful only to muscle and not to bone (=subset *C* in Fig. 1). For example, bones seem to require comparatively few repetitions for force peaks to saturate as a stimulus [11, 14]. On the other hand, while dietary protein supplementation is a powerful stimulus for the accrual of muscle mass [15], it seems that only very substantial dietary protein deficits are detrimental to bone [16].

The crucial question, of course, is under which conditions muscles develop their maximal force and tension. For single fibers, this is quite clearly the case during maximal eccentric contractions [17], i.e., when a muscle is maximally activated and contracting, but overwhelmed by the external opposing force and thus forced into lengthening. In humans, however, the enhancement of force generation during eccentric contraction seems much less impressive than when testing single muscle fibers [18, 19]. Several explanations could apply for this discrepancy between cellular level and the level of the human, ranging from difficulties that people have to perform eccentric test

contractions, up to the very limited understanding of muscle mechanics on the mesoscopic level (i.e., between the level of single fibers and the level of individual muscles). In any case, it seems reasonable to assume that however our muscles may produce their peak forces, it will be in direct relationship to their cross-sectional area.

Muscle Volume as a Surrogate for Muscle Power

Let us turn to the third dimension. Mechanical power is the product of force and velocity ($P = F{\cdot}v$). Thus, the greater the velocity of a muscle contraction, the lower is the force that a muscle can develop. We can, in an experiment of thought, explore how muscle volume and CSA relate to power and force-generating capacity (see Fig. 4a). Clearly, the contraction of muscle cells is ultimately caused by the power stroke of the myosin heavy chain. The capacity of a given muscle to generate force and power is therefore defined by the total number of sarcomeres n. If all sarcomeres were aligned in parallel (case A in Table 1), then the muscle's velocity would coincide with that of a single sarcomere, but all sarcomeres would add up to yield the muscle's force. If, conversely all of these n sarcomeres were aligned in a long chain (Table 1, case B), i.e., if the CSA were to be minimized and the length were maximized, then force F would be that of a single sarcomere, and the muscles velocity would be the sum of the sarcomeres' velocities. The number of sarcomeres in series (n_{Series}) therefore generally defines the maximum velocity of a muscle. Accordingly, long muscles can generate faster contractions than short muscles. Conversely, muscles with greater CSA produce greater forces than muscles with small CSA.

Notably, the muscle's power generation simply depends on the number of sarcomeres n, regardless of how many of them are aligned in series and how many in parallel. The muscle's volume therefore directly relates to its capacity to generate power.

Muscle Architecture

To make things more complicated, and realistic, we now have to consider muscle architecture. As illustrated in Fig. 4b, the direction of a muscle's fascicles is often not directly aligned with its gross anatomical orientation. This results in a reduction in the force that is transmitted from the fascicle onto the aponeurosis and tendon, the degree of which scales with the cosine of pennation angle α [20]. The small reduction in transmitted force from each fascicle is reversed by the great number of serial fascicles in a pennated muscle, which adds many sarcomeres in parallel to the effective cross-section. Thus, pCSA is in reality greater than aCSA for most muscles. Of note, pennation angle α typically increases in muscle hypertrophy, and it decreases in atrophy [21].

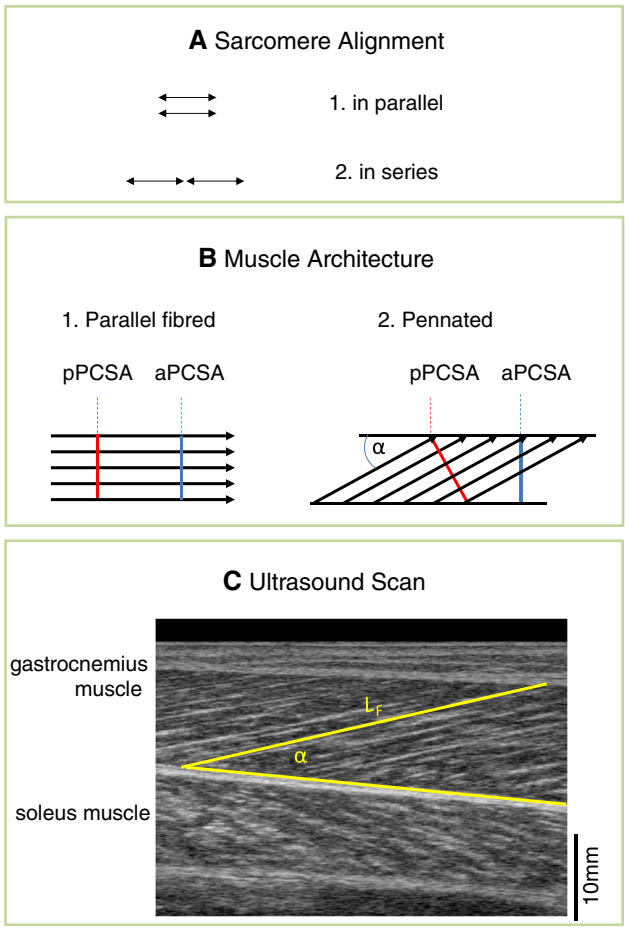

Fig. 4 Macroscopic arrangement of muscles, and how this affects their mechanics. **a** Sarcomeres in parallel add their forces, while sarcomeres in series add their velocities. **b** The anatomical CSA (aCSA) is defined as the cross-section perpendicular to a muscle's macroscopic alignment. The physiological CSA (pCSA) of a muscle is defined of the cross-section that is perpendicular to the sum of all fascicles. aCSA and pCSA therefore only coincide when the fascicles are parallel with the macroscopic alignment. In most muscles this is not the case, however, as in the various forms of pennated muscles, and aCSA and pCSA differ from each other. **c** Ultrasound scan of the medial gastrocnemius muscle and the underlying soleus muscle (*image* courtesy Kirsten Albracht). The parallel "streaks" are related to the muscles' fascicules and therefore allow assessment of muscle architecture, meaning fascicle length L_F and pennation angle α

It has to be considered, though, that the model for the pennated muscle in Fig. 4b is mechanically unstable: The whole architecture would collapse if a pull was exerted along the fibers without a matching force perpendicular to the fiber orientation. While it is currently not understood how muscles stabilize their architecture during contractions, researchers still assess muscle architecture by ultrasound, either at rest or during contractions, as depicted in Fig. 4c. From such examinations, the muscle's pCSA can

Table 1 Muscle dimensions and mechanics

	F_{Muscle}	V_{Muscle}	P_{Muscle}
(A) Parallel alignment	$n \cdot F_{Sarcomere}$	$v_{Sarcomere}$	$n \cdot v_{Sarcomere} \cdot F_{Sarcomere}$
(B) Serial alignment	$F_{Sarcomere}$	$n \cdot v_{Sarcomere}$	$n \cdot v_{Sarcomere} \cdot F_{Sarcomere}$
(C) General case	$N_{Parallel} \cdot F_{Sarcomere}$	$N_{Series} \cdot v_{Sarcomere}$	$n \cdot v_{Sarcomere} \cdot F_{Sarcomere}$

In theory, the force of a muscle (F_{Muscle}) is defined by the number of sarcomeres in parallel ($n_{Parallel}$) multiplied with each sarcomere's force ($F_{Sarcomere}$), while its velocity of contraction (v_{Muscle}) is given by the number of sarcomeres in series (n_{Series}) multiplied by the velocity of each sarcomere ($v_{Sarcomere}$). This can be deduced from the two extreme cases of (A) parallel alignment (Fig. 4a1), where $n = n_{Parallel}$ and (B) serial alignment (Fig. 4a2), where $n = n_{Series}$. Notably, the power (P_{Muscle}) only depends on the number of sarcomeres (n), regardless of the anatomical arrangement—at least in theory

then be computed by dividing the muscle's volume by its fascicle length.

Muscles Generate Force and Torque

Although muscles primarily generate force along their anatomical axis, joints "translate" this linear force into a rotatory actuation. Therefore, the external effect of a muscles force is a torque, described by $T = F \cdot a$, where T, is the torque produced, F is the force that caused it, and a is the lever arm (see Fig. 5). That equation can also be used to assess the muscle force F by dividing the measured torque T by the lever arm a. Virtually, all of our muscles work against poor levers. This is helpful in that it (1) generates movements and movement speeds that are greater in the actuated limbs than in the actuating muscles themselves, and (2) bending moments imposed by the musculature are comparatively minimized. Yet, the mere fact that muscles' lines of action almost never pass the joints' centers of rotation proves that muscles do exert bending moments upon the bones they actuate.

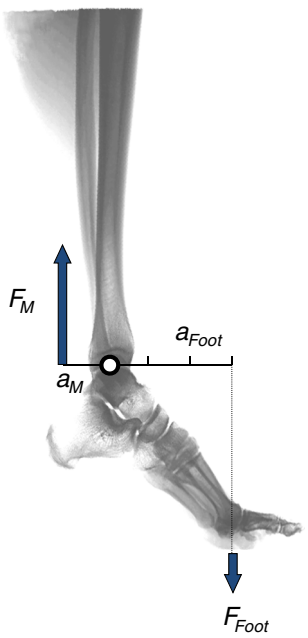

Fig. 5 Illustration of how the lever rule applies to the human ankle. The ankle torque T rotates the foot around the ankle. The calf muscles generate muscle force F_M, which is transmitted to the heel bone via the Achilles tendon. The lever arm a_M is the distance perpendicular from the force vector F_M to the ankle's center of rotation. Ankle torque $T = F_M \cdot a_M$. Under static conditions, $T = -F_{Foot} \cdot a_{Foot}$, Thus, since $a_{Foot} = 3 \cdot a_M$, F_M is three times as great as F_{Foot}. Generally, forces inside our musculoskeletal system are significantly greater than forces we can transmit to the outside world. Diagram adopted from [9]

As bone adapts to compressive *and* bending loads, it is therefore important to compare appropriate variables from muscle and bone with each other. From a physical point of view, plotting bone CSA versus muscle CSA would be appropriate for the force component of bone loading. This should primarily be done at such bone sites that are little affected by bending and torsion, but rather loaded in compression, such as the distal tibia at 15 % of its length [22].

To investigate adaptation to bending and torsion, one would have to compare bone axial and polar CSMIs, respectively, with the moments induced by muscle contractions—a task that is inherently difficult. A previous study has successfully quantified the muscle bending moment as the product of tibia length and gross muscle CSA at 66 % of the tibia length, i.e., where muscle CSA is greatest [23].

Complexity of the Musculature

To make things even more complicated, we now have to consider also that most of our joints are actuated by more than one muscle. In fact, for most joint movements (e.g., foot plantar flexion) there are several muscles that work synergistically (e.g., soleus, gastrocnemius, peronei and tibialis posterior muscles) and several muscles can work antagonistically against the agonists. The amount of torque and compression that each of these muscles exerts depends on its anatomical orientation and dimensions. Teasing out the exact mechanical interactions of such synergistic groups is cumbersome and scientifically yet unaccomplished. The fact

that the relative contribution of a single muscle to a limb's musculature depicts great interindividual variation does not make the task of high-fidelity modeling of the muscular mechanics any easier. Thus, if each muscle was to be activated in an independent fashion, then they would impose highly complex strain patterns on bones, which would constitute major problems for muscle–bone imaging.

However, some of that complexity is relaxed by the occurrence of co-contractions. These are contractions in which synergistic and antagonistic muscle groups contract more or less simultaneously [24], the result being an increase in joint stiffness. Stiffness is important in ballistic movements and helps to store energy in running and hopping by antagonistic pre-activation [25]. Control of joint stiffness is thus an important constituent of motor control in complex patterns of movement, including locomotion, and it is enabled by a specific cortical control system that is distinct from the system that controls joint movement [26]. It is important here that co-contractions enhance reflex stiffness [27], and that co-contractions, and thus joint stiffness, increase during forceful dynamic movements [28]. In summa, there is good evidence to support the assumption of a co-contracting musculature in those habitual activities that generate greatest forces and thus bone loads. However, however reasonable that assumption may be, it remains an assumption in the absence of direct evidence.

Imaging Approaches

The four imaging techniques that are broadly available to scan muscles are summarized in Table 2 (see also Fig. 6). As can be seen from that Table, there is no standard technique that can assess muscle volume, CSA and architecture of single muscles at the same time, although three-dimensional ultrasound is an interesting approach that might do this in future [29]. Of these four techniques, DXA is the least informative, but its estimate of fat-free mass is a quick and useful surrogate for muscle volume or muscle mass (MM). CT technology does provide accurate measurements of muscle CSA, and image stacks can then yield muscle volume. However, it is difficult to obtain such image stacks with current pQCT machines. Likewise, neither CT nor pQCT allow for differentiation of individual muscles, so that only gross muscle cross-sections can be reported that comprise all muscles within the section image. MR imaging is much

Table 2 Imaging techniques for muscle

	DXA	CT	MRI	Ultrasound
Muscle volume	Yes	Yes (from stacks)	Yes	No (not routinely)
Muscle CSA	No	Yes	Yes	Yes (in principle)
Individual muscles	No	No	Yes (often)	Yes
Muscle architecture	No	No	No (not yet)	Yes

No single technique can assess muscle volume, CSA and architecture at the same time. Therefore, high-fidelity approaches will typically combine ultrasound as the most refined measurement with MRI, as the latter is best suited to objectively assess CSA and volume of single muscles or at least muscle groups. The beauty of pQCT-derived muscle CSA measurements is that they often come "for free" with the bone scan. DXA, although not very refined, still constitutes a rapid assessment of muscle bulk

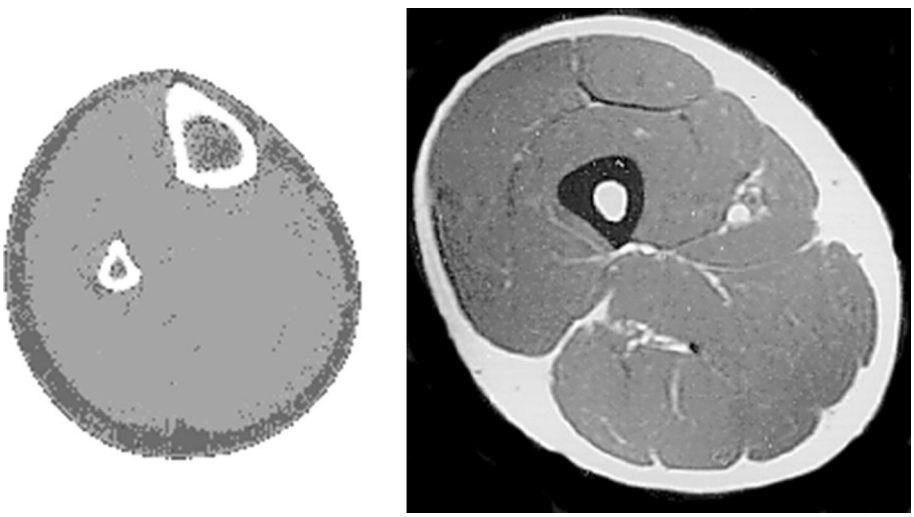

Fig. 6 Comparison of pQCT (*left*, human shank) and MRI (*right*, human thigh) images. pQCT normally allows only definition of the gross muscle CSA in a limb, while MRI allows to differentiate muscle groups or even individual muscles

more elegant here, albeit at the expense of human labor involved in image analysis. Depending on image resolution and abundance of intermuscular connective tissue, one can often discern single muscles on good quality MR images. Ultrasound can provide high-resolution images of even small single muscles, and the streaks on axial scans reflect the muscle architecture. However, ultrasound imaging is depending on the sonographer and is thus less objective than other imaging techniques. Moreover, it is not straightforward to assess muscle CSA, in particular for larger muscles. Therefore, ultrasound imaging will normally be an "add-on" for the study of muscle–bone interactions and should normally be combined with MR imaging or at least CT approaches. In addition to these standard techniques, MR diffusion imaging offers an interesting opportunity to assess muscle volume and fiber orientation in one testing session [30]—a novel approach that awaits to be used in the field of muscle–bone imaging.

Imaging Muscle "Quality"

As stated above, muscle mechanical output is a consequence of the actin–myosin cross-bridge cycle. Therefore, in any given muscle volume or CSA, it will ultimately be the number of active cross-bridges that defines mechanical output. Myosin concentration in single muscle fibers declines both in aging and after immobilization [31], suggesting that the intrinsic strength of muscles is affected by age and habitual muscle exercise. Moreover, at the microscopic level, it is now known that lipids accumulate in muscle diseases [32] and aging [33]. It is therefore clear that increases in intra- and intermuscular lipid concentration must reduce the abundance of cross-bridges, and similar arguments could be made about the general increase in intra- and intermuscular connective tissue that becomes more abundant with old age.

The idea should therefore be to visualize muscle "quality" as an indicator of its mechanical competence. A simplistic approach, with demonstrated merits [34, 35] and pitfalls [36] consists in using muscle X-ray absorption (sometimes called muscle "density"). However, one needs to consider that there is currently no approach to directly assess the abundance of cross-bridges in the muscle, and that all previous approaches to muscle "quality" are therefore rather indirect, at least when we think of quality in relation to force-generating capacity. It is therefore unclear, in how far "quality" approaches can improve muscle–bone imaging approaches.

Identifying Muscle–Bone Relationships

Coming to the final step in the logistics, the above normative and theoretical considerations must be put onto an empirical bases. Notably, out of the many different approaches that are theoretically possible, only a subset of image-based muscle–bone relationships will make sense from a physical viewpoint. Therefore, the identification of meaningful muscle–bone relationships has to follow the principles outlined above. This section summarizes the most popular and promising approaches that have been used in the past.

1. Bone mass versus muscle mass

Plotting BMC against MM may look questionable at first glance. Is it not the case that MM relates to power, rather than to force, and is it not the case that BMC is not directly linked to bone strength or stiffness? And yet, within the same limb, muscle and bone masses can become "normalized" through the limb's length (L): MM divided by L yields the mean CSA of the muscle, and BMC divided by L yields the mean CSA of the bone. In this sense, the MM:BMC ratio is equivalent to the CSA ratio of muscle and bone—which is the meaningful MBSI for the bone's adaptation to compression loading.

Along this line of reasoning, several DXA studies have described linear relationships between BMC and MM in the human body [37, 38]. Quite interestingly, these plots revealed distinct group differences, with similar slopes but increasing intercepts for children < [men + post-MP women] < pre-MP women (see Fig. 7) [38]. Over the natural, anthropometric associations between muscles and bones, these findings express the existence and function of the same *mechanostat* system in *Homo* regardless of sex and age, and the (positive) natural modulation exerted by sex hormones on the system.

2. Bone and muscle CSA ratio

Comparing bone and muscle, CSA is the straightforward way of assessing a bone's adaptation to compression, which has been done by many authors [23, 39, 40]. Doing so, it is common practice to assess muscle CSA where it is largest, which seems straightforward. Less attention has been paid to selection of the bone site. However, when considering that alongside with compression bones are simultaneously subjected to torsion and bending (Yang et al. in preparation), one has to consider that the specific mechanical environment may vary even within a given bone. Taking the human tibia as an example, one can think of it as being composed by three different regions with quite different function: A distal region in which compression predominates, a central region that is adapted to bending and torsion, and a proximal region where "splitting-up" the force onto the two knee condyles dictates the design [22]. Accordingly, one ought to select a distal tibia site in order judge compression muscle–bone interaction, and indeed, correlation coefficients between muscle CSA

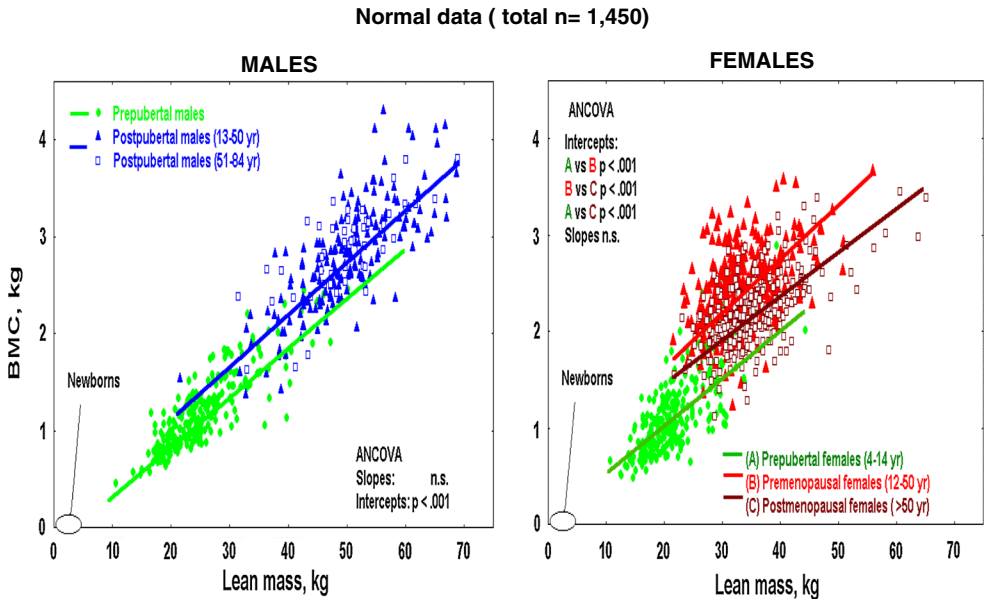

Fig. 7 Plotting DXA-based assessments of total body BMC versus total body lean mass in 1,450 people yielded close correlation between both variables, and similar slopes but different intercepts that varied with gender and pubertal and menopausal state [38]

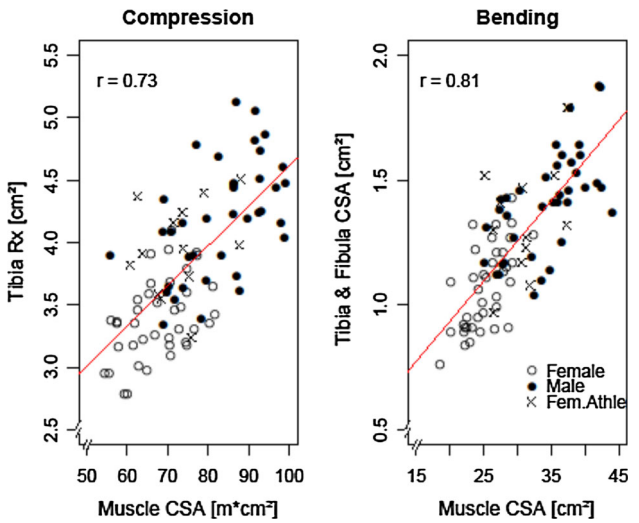

Fig. 8 Comparison of two different muscle–bone strength indices (MBSI), for compression and for bending, respectively, assessed at the distal tibia at 33 % of its length of young healthy women and men, and a group of female elite volleyball players. Based on the closer relationship, the bending MBSI seems a better descriptor. For details, see [23]

and bone CSA seem to be greater for the distal than for the central or proximal tibia region [23]. Another fruitful approach to study for compressive muscle–bone interaction is to isolate sectors within the tibia CSA that are thought to be loaded specifically in compression [40].

3. Modeling bending and torsion

Going more "mechanical," some pQCT studies have tried to consider bending and torsion as important loading modes. For the regional muscles, this could be done e.g., by using the product of limb length and regional muscles as a surrogate for bending loads (see above). As judged by Pearson's correlation coefficients, that "muscle bending moment" was closer related to the tibia's CSMI than the compression MBSI at the same anatomical site [23], suggesting that bending seems to be a more important determinant for bone adaptation than compression, at least for the mid-tibia (see Fig. 8).

It is important, however, that bone bending and torsion is not only caused by regional muscles, but also by muscles that actuate neighboring and even distant segments. For the tibia, for example, the knee extensors create a bending moment that increases when we flex our knees. Thus, while tibia loading will be dominated by the plantar flexors during hopping with straight knees, it will receive a significant bending load from the thigh muscles during standing up and jumping from deep squats. This view has recently been confirmed by a study that reported closer muscle–bone relationships between thigh muscles and tibia than between the tibia and its regional muscles [41].

As to torsion, a recent study in elite youth tennis players concluded that the twisting forearm movements in tennis playing was the most likely explanation for the greater bone CSA and CSMI on the racket forearm, as compared to the other side [42]. Likewise for the humerus, and as in throwers [43], torsion seems to be the salient mode of loading in tennis. However, it is clear from the upper arms' anatomy that they do not generate humerus torsion themselves, but can only help to increase the arm's moment of resistance in torsional movements by flexing the elbow.

Table 3 Diagnostic approach

Muscle mass and strength	Bone:muscle ratio	
	Normal	Abnormal
Normal	Normal finding	Bone disorder
Abnormal	Muscle disorder	Mixed disorder

Combining information from bone and muscle allows differentiation of primary bone disorders (e.g., low BMC, but normal muscle mass and strength and thus low bone:muscle ratio) and primary muscle disorders (e.g., low muscle mass and strength, but normal bone:-muscle ratio and thus low BMC). In the first step, one regards whether muscle mass and strength are normal or abnormal. In case of abnormal values, an abnormal bone:muscle ratio then suggests an abnormal BMC due to an disrupted adaptation of bone. Of note, this scheme is only applicable when muscle mass and strength are in proportion. In some disorders, such as Duchenne's dystrophy or myostatin mutations, this is not the case and the scheme will therefore not apply

Thus, although there is a close muscle–bone relationship between the upper arm muscle CSA, the slope of that relationship was almost 1.5 times larger in the racquet arm, clearly demonstrating that not regional muscles, but probably the nonregional shoulder rotators are the cause of the bigger humerus in the racquet arm.

Interpreting Muscle–Bone Strength Indices

Text book definitions of osteoporosis compare an individual's bone mass indicator (often DXA-based areal bone mineral density is used) to a reference population in order to determine whether that person has reduced bone mass and thus bone strength [44]. However, such an approach will not be able to distinguish between primary bone disorders, i.e., such disorders where all stimuli to the bone are adequate but bone responds in an inadequate way, from secondary bone disorders, i.e., such disorders where the stimuli to the bone are inadequate in the first place. A diagnostic algorithm proposed by Schönau and co-workers solves this issue in an elegant way [45, 46]. This algorithm is illustrated in Table 3. As can be seen from the Table, a primary bone disorder is characterized by a BMC that is low for body size or age, and also a low bone:muscle ratio. A primary muscle disorder, by contrast, is associated with reduced muscle size, but normal bone:muscle ratio, which then secondarily causes the reduction in BMC. This approach is nowadays used in the field of pediatric medicine, and it should also be applicable in other fields of medicine. Thus, it has been shown that post-menopausal women with low muscle mass and low bone:muscle ratio have a particularly high risk of osteoporotic fracture [47]—a finding with which many clinicians will concur, but which has been poorly understood.

Conclusion

Bone scanning techniques, such as QCT and pQCT can predict bone function in terms of strength and stiffness with good accuracy. This contrasts with the assessment of muscle size, volume and architecture by CT approaches, MR imaging and ultrasound that currently allow only crude predictions of habitual bone loading by the musculature. The fact that even such crude predictions yield information that is useful for clinical medicine underlines the principle fruitfulness of muscle–bone imaging. It must be anticipated that future improvements in the field of muscle scanning will improve the validity of that kind of information.

Disclosures

Conflict of interest Jörn Rittweger, José-Luis Ferretti declare that they have no conflict of interest.

Animal/Human Studies This review does not contain any studies with human or animal subjects performed by any of the authors.

References

1. Thompson DA. On growth and form. Cambridge: Cambridge University Press; 1917.
2. Frost HM. Bone "mass" and the "mechanostat": a proposal. Anat Rec. 1987;219(1):1–9.
3. Ferretti JL, Capozza RF, Zanchetta JR. Mechanical validation of a tomographic (pQCT) index for noninvasive estimation of rat femur bending strength. Bone. 1996;18(2):97.
4. Martin DE, Severns AE, Kabo JM. Determination of mechanical stiffness of bone by pQCT measurements: correlation with non-destructive mechanical four-point bending test data. J Biomech. 2004;37:1289–93.
5. Currey JD. Effects of differences in mineralization on the mechanical properties of bone. Philos Trans R Soc Lond B Biol Sci. 1984;304(1121):509.
6. Gordon JE. Science of structures and materials. New York: WH Freeman & Co; 1988.
7. Ferretti JL, Schiessl H, Frost HM. On new opportunities for absorptiometry. J Clin Densitom. 1998;1(1):41.
8. Capozza RF, Rittweger J, Reina PS, Mortarino P, Nocciolino LM, Feldman S, et al. pQCT-assessed relationships between diaphyseal design and cortical bone mass and density in the tibiae of healthy sedentary and trained men and women. J Musculoskelet Neuronal Interact. 2013;13(2):195–205 Epub 2013/06/04.
9. Maganaris CN, Rittweger J, Narici MV. Adaptive Processes in Human Bone and Tendon. In: Cardinale M, Newton R, Nosaka K, editors. Strength and conditioning biological principles and practical applications. Oxford: Wiley; 2011. p. 137–47.
10. McArdle WD, Katch FI, Katch VL. Muscular strength: training muscles to become stronger. Exercise physiology. Philadelphia: Lippincott Williams & Wilkins; 2001. p. 500.
11. Rubin CT, Lanyon LE. Kappa Delta Award paper. Osteoregulatory nature of mechanical stimuli: function as a determinant for adaptive remodeling in bone. J Orthop Res. 1987;5(2):300–10.
12. Mosley JR, March BM, Lynch J, Lanyon LE. Strain magnitude related changes in whole bone architecture in growing rats. Bone. 1997;20(3):191.

13. Mosley JR, Lanyon LE. Strain rate as a controlling influence on adaptive modeling in response to dynamic loading of the ulna in growing male rats. Bone. 1998;23(4):313–8.
14. Umemura Y, Ishiko T, Yamauchi T, Kurono M, Mashiko S. Five jumps per day increase bone mass and breaking force in rats. J Bone Miner Res. 1997;12(9):1480.
15. Rennie MJ, Wackerhage H, Spangenburg EE, Booth FW. Control of the size of the human muscle mass. Annu Rev Physiol. 2004;66:799–828.
16. Ammann P, Laib A, Bonjour JP, Meyer JM, Ruegsegger P, Rizzoli R. Dietary essential amino acid supplements increase bone strength by influencing bone mass and bone microarchitecture in ovariectomized adult rats fed an isocaloric low-protein diet. J Bone Miner Res. 2002;17(7):1264–72.
17. Hill AV. The heat of shortening and dynamic constants of muscle. Proc R Soc Lond Ser B. 1938;126:136.
18. Westing SH, Seger JY, Karlson E, Ekblom B. Eccentric and concentric torque-velocity characteristics of the quadriceps femoris in man. Eur J Appl Physiol Occup Physiol. 1988;58(1–2):100–4 Epub 1988/01/01.
19. Wilhite MR, Cohen ER, Wilhite SC. Reliability of concentric and eccentric measurements of quadriceps performance using the KIN-COM dynamometer: the effect of testing order for three different speeds. J Orthop Sports Phys Ther. 1992;15(4):175–82 Epub 1992/01/01.
20. Narici MV, Binzoni T, Hiltbrand E, Fasel J, Terrier F, Cerretelli P. In vivo human gastrocnemius architecture with changing joint angle at rest and during graded isometric contraction. J Physiol. 1996;496(Pt 1):287–97 Epub 1996/10/01.
21. Seynnes OR, de Boer M, Narici MV. Early skeletal muscle hypertrophy and architectural changes in response to high-intensity resistance training. J Appl Physiol. 2007;102(1):368–73.
22. Capozza R, Feldman S, Mortarino P, Reina P, Schiessl H, Rittweger J, et al. Structural analysis of the human tibia by tomographic (pQCT) serial scans. J Anat. 2010;216:470–81.
23. Rittweger J, Beller G, Ehrig J, Jung C, Koch U, Ramolla J, et al. Bone-muscle strength indices for the human lower leg. Bone. 2000;27(2):319–26.
24. Tilney F, Pike FH. Muscular coordination experimentally studies in its relation to the cerebellum. Arch Neurol Psychiatr. 1925;13:289–309.
25. Hobara H, Kanosue K, Suzuki S. Changes in muscle activity with increase in leg stiffness during hopping. Neurosci Lett. 2007;418(1):55–9 Epub 2007/03/21.
26. Humphrey DR, Reed DJ. Separate cortical systems for control of joint movement and joint stiffness: reciprocal activation and coactivation of antagonist muscles. Adv Neurol. 1983;39:347–72 Epub 1983/01/01.
27. Carter RR, Crago PE, Gorman PH. Nonlinear stretch reflex interaction during cocontraction. J Neurophysiol. 1993;69(3):943–52 Epub 1993/03/01.
28. Hagood S, Solomonow M, Baratta R, Zhou BH, D'Ambrosia R. The effect of joint velocity on the contribution of the antagonist musculature to knee stiffness and laxity. Am J Sports Med. 1990;18(2):182–7 Epub 1990/03/01.
29. Barber L, Barrett R, Lichtwark G. Validation of a freehand 3D ultrasound system for morphological measures of the medial gastrocnemius muscle. J Biomech. 2009;42(9):1313–9 Epub 2009/04/21.
30. Galban CJ, Maderwald S, Uffmann K, de Greiff A, Ladd ME. Diffusive sensitivity to muscle architecture: a magnetic resonance diffusion tensor imaging study of the human calf. Eur J Appl Physiol. 2004;93(3):253–62 Epub 2004/08/24.
31. D'Antona G, Pellegrino MA, Adami R, Rossi R, Carlizzi CN, Canepari M, et al. The effect of ageing and immobilization on structure and function of human skeletal muscle fibres. J Physiol. 2003;552(Pt 2):499–511.
32. Jones DA, Round JM, Edwards RH, Grindwood SR, Tofts PS. Size and composition of the calf and quadriceps muscles in Duchenne muscular dystrophy. A tomographic and histochemical study. J Neurol Sci. 1983;60(2):307–22.
33. Taaffe DR, Henwood TR, Nalls MA, Walker DG, Lang TF, Harris TB. Alterations in muscle attenuation following detraining and retraining in resistance-trained older adults. Gerontology. 2009;55(2):217–23 Epub 2008/12/09.
34. Visser M, Kritchevsky SB, Goodpaster BH, Newman AB, Nevitt M, Stamm E, et al. Leg muscle mass and composition in relation to lower extremity performance in men and women aged 70 to 79: the health, aging and body composition study. J Am Geriatr Soc. 2002;50(5):897–904 Epub 2002/05/25.
35. Lang T, Cauley JA, Tylavsky F, Bauer D, Cummings S, Harris TB. Computed tomographic measurements of thigh muscle cross-sectional area and attenuation coefficient predict hip fracture: the health, aging, and body composition study. J Bone Miner Res. 2010;25(3):513–9 Epub 2010/04/28.
36. Rittweger J, Moller K, Bareille MP, Felsenberg D, Zange J. Muscle X-ray attenuation is not decreased during experimental bed rest. Muscle Nerve. 2013;47(5):722–30 Epub 2013/03/23.
37. Schiessl H, Frost HM, Jee WS. Estrogen and bone-muscle strength and mass relationships. Bone. 1998;22(1):1–6.
38. Ferretti JL, Capozza RF, Cointry GR, Garcia SL, Plotkin H, Alvarez Filgueira ML, et al. Gender-related differences in the relationship between densitometric values of whole-body bone mineral content and lean body mass in humans between 2 and 87 years of age. Bone. 1998;22(6):683.
39. Schoenau E, Neu CM, Mokov E, Wassmer G, Manz F. Influence of puberty on muscle area and cortical bone area of the forearm in boys and girls. J Clin Endocrinol Metab. 2000;85(3):1095.
40. Heinonen A, McKay HA, Whittall KP, Forster BB, Khan KM. Muscle cross-sectional area is associated with specific site of bone in prepubertal girls: a quantitative magnetic resonance imaging study. Bone. 2001;29(4):388–92 Epub 2001/10/12.
41. Rantalainen T, Nikander R, Kukuljan S, Daly RM. Mid-femoral and mid-tibial muscle cross-sectional area as predictors of tibial bone strength in middle-aged and older men. J Musculoskelet Neuronal Interact. 2013;13(3):235–44 Epub 2013/08/31.
42. Ireland A, Maden-Wilkinson T, McPhee J, Cooke K, Narici M, Degens H, et al. Upper limb muscle–bone asymmetries and bone adaptation in elite youth tennis players. Med Sci Sports Exerc. 2013;45(9):1749–58 Epub 2013/03/12.
43. Bogenschutz ED, Smith HD, Warden SJ. Midhumerus adaptation in fast-pitch softballers and the effect of throwing mechanics. Med Sci Sports Exerc. 2011;43(9):1698–706 Epub 2011/02/12.
44. Lindsay R, Cosman F, Harrison TR, Kasper D, Braunwald E, Fauci A, et al. Ostoporosis. Harrison's principles of internal medicine. New York: Mc Graw-Hill; 2004. p. 2226.
45. Schonau E, Schwahn B, Rauch F. The muscle–bone relationship: methods and management—perspectives in glycogen storage disease. Eur J Pediatr. 2002;161(Suppl 1):S50.
46. Schönau E, Fricke O. Muscle and bone: a functional unit. Deutsches Aerzteblatt. 2006;103(50):A3414–9.
47. Capozza RF, Cure-Cure C, Cointry GR, Meta M, Cure P, Rittweger J, et al. Association between low lean body mass and osteoporotic fractures after menopause. New York, NY: Menopause; 2008.